

Limits of metastability in amorphous ices: ²H-NMR relaxation

Cite this: *Phys. Chem. Chem. Phys.*,
2013, **15**, 576

Florian Löw,^{*a} Katrin Amann-Winkel,^b Burkhard Geil,^c Thomas Loerting,^b
Carolin Wittich^a and Franz Fujara^a

The high-frequency reorientation dynamics of O–²H bonds is investigated in various amorphous ices including eHDA (expanded high density amorphous ice), LDA-II (low density amorphous ice II) and HGW (hyperquenched glassy water) using ²H-NMR spin–lattice relaxation as a local probe. Both low density forms, HGW and LDA-II, show similar spin–lattice relaxation but differ in the thermal stability with respect to the transition into crystalline cubic ice I_c. HGW already transforms slightly above 135 K whereas LDA-II crystallizes at 150 K. eHDA is distinguishable from other high density amorphous ices in its thermal stability and spin–lattice relaxation. Its relaxation times are much larger compared to those of VHDA (very high density amorphous ice) and uHDA (unrelaxed high density amorphous ice). eHDA does not show annealing effects, transforms sharply into LDA-II above 123 K and provides higher thermal stability as compared to other high density forms.

Received 8th October 2012,
Accepted 19th November 2012

DOI: 10.1039/c2cp43543h

www.rsc.org/pccp

1. Introduction

This paper is the second part of a twin publication. For a general introduction into the current debate on the nature and the physical properties of amorphous ices we refer to the first part¹ which discusses questions of metastability in context with neutron scattering experiments. Here, instead, we give a short summary of this debate:

There are several disordered or amorphous low temperature states of solid water. The finding of a high density form formed by application of high pressures triggered many theoretical and experimental investigations of the physical nature of amorphous ices. A first-order-like transition between low (LDA) and high density amorphous ice (HDA) under pressure has been found by Mishima.² In some models LDA and HDA are regarded as the glassy proxies of two ultraviscous, deeply supercooled liquids.^{3,4} However, the phase transition between the different disordered forms has mainly been studied at ambient pressure and not at pressures around the estimated equilibrium phase boundary at ≈ 200 MPa.² Nowadays, the conversion from the high to the low density form is understood as an annealing process of the high density structure followed

by a first-order transition.^{5–8} The obtained low density state can be further annealed,^{6,9} a circumstance that has been rarely considered in the literature. While annealing of the high density structure leads to various forms related to HDA (VHDA,^{10,11} eHDA,¹² uHDA¹³ and rHDA¹³), the annealing at the low density side of the transition tunes the properties of LDA without changing its density.^{9,14,15} In the following we will distinguish between LDA-I obtained by isobaric warming of uHDA at ambient pressure and LDA-II obtained by isothermal decompression of VHDA at 143 K.^{9,14,16}

In a ²H NMR study Scheuermann *et al.*¹⁷ discussed spin–lattice relaxation experiments on uHDA, VHDA, LDA and crystalline cubic ice I_c. Both low density forms have been obtained by isobaric warming at ambient pressure. The various ice states can clearly be identified by their relaxation times T_1 , as already proposed by Ripmeester *et al.*¹⁸ However, strong scatter in $T_1(T)$ scans among various samples was found,¹⁷ which has been explained by history dependent properties of amorphous ices. During the transformation of VHDA into LDA an intermediate HDA stage has been found. Those findings, reported in ref. 17, are in agreement with neutron scattering studies on structural and dynamical properties of amorphous ices.⁸

In this paper, we present ²H NMR T_1 data of the low density forms, LDA-II and hyperquenched glassy water (HGW),^{19,20} as well as the high density form eHDA, thereby extending the study of Scheuermann *et al.*¹⁷ It is well known that spin–lattice relaxation is sensitive to fast, large as well as small angle

^a Institut für Festkörperphysik, Technische Universität Darmstadt, Hochschulstr. 6,
64289 Darmstadt, Germany. E-mail: florian.loew@physik.tu-darmstadt.de

^b Institute of Physical Chemistry, University of Innsbruck, Innrain 52a, A-6020
Innsbruck, Austria

^c Institut für Physikalische Chemie, Georg-August-Universität Göttingen,
Tammanstr. 6, 37077 Göttingen, Germany

molecular reorientations. Therefore, T_1 is expected to probe changes in the short range order and hypothetical dynamic anomalies close to the glass transition temperature. We will show that HGW has a $T_1(T)$ dependence similar to both low density amorphous ices LDA-I and LDA-II, whereas $T_1(T)$ of eHDA differs from that of other high density states.

2. Experimental

The samples were prepared from $^2\text{H}_2\text{O}$ (99.9% deuteration) purchased from *eurisotop*. The preparation techniques are described in detail by Mayer¹⁹ and Winkel *et al.*¹⁴ Hyperquenched glassy water (HGW) was obtained by deposition of micrometer-sized water droplets on a copper plate at 84 K inside a vacuum chamber at $p \approx 6 \times 10^{-4}$ mbar yielding cooling rates of up to 10^7 K s⁻¹. The HGW sample was annealed at 130 K for 90 min.

The other amorphous ices were obtained after isothermal compression of I_h at 110 K followed by heating to 160 K at a pressure of 1.1 GPa. The VHDA, obtained in this way, was then decompressed isothermally at 143 K with a rate of 13 MPa min⁻¹ to $p \approx 90$ MPa towards eHDA or further down to $p \approx 8$ MPa towards LDA-II. In both cases, the decompression was followed by quenching to 77 K. Powder X-ray diffractograms were taken to confirm the X-ray amorphous nature of the samples. Care was taken not to exceed 85 K when transferring them into the flow cryostat of the NMR spectrometer. The temperature stability is estimated to be ± 0.5 K over several days.

The experiments were performed at a deuteron Larmor frequency of 46.7 MHz. Strong rf pulses (with $\pi/2$ pulse lengths of about 2.0 μs) were applied to ensure the full excitation of the broad deuteron powder Pake spectra.

^2H -NMR relaxation is an excellent tool for the study of O- ^2H bond reorientations on a timescale of the inverse Larmor frequency.²¹ Amorphous systems exhibit a broad heterogeneous distribution of spin-lattice relaxation times T_1 leading to a glass-typical nonexponential magnetization recovery (Fig. 1), which is often parameterized by a stretched-exponential function (Kohlrausch law):

$$M(t) = M_0 \left(1 - \exp \left[- \left(\frac{t}{T_1} \right)^\beta \right] \right). \quad (1)$$

T_1 is the spin-lattice relaxation time and β the stretching parameter (also called Kohlrausch parameter).

3. Results and discussion

For the various amorphous ices, we sampled magnetization recovery curves like the one shown in Fig. 1 for many temperatures, stepwise. All data $M(t)$ stem from the amplitude of solid echos; the variable t being the delay between an initial saturation pulse sequence and the solid echo two pulse sequence. The Fourier transforms of the echoes are broad powder Pake spectra parametrized by quadrupole coupling parameters $e^2qQ/h = (224.6 \pm 2.2)$ kHz and $\eta = (0.105 \pm 0.005)$ for eHDA and

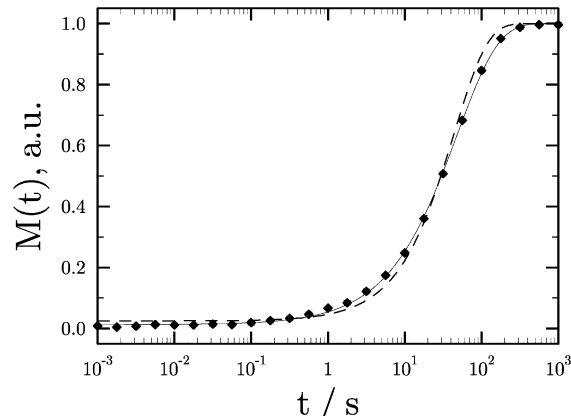


Fig. 1 A typical magnetization recovery curve covering six orders of magnitude in time of a LDA-II sample at 134.2 K. The fit (solid line) corresponds to $\beta = 0.81 \pm 0.01$ and $T_1 = (48.3 \pm 0.9)$ s. For comparison, the dashed line represents a monoexponential parametrization.

$e^2qQ/h = (217.9 \pm 1.5)$ kHz and $\eta = (0.109 \pm 0.003)$ for LDA-II in agreement with ref. 18 which show no indication of motional narrowing.

3.1 Thermal stability of amorphous ices

Our experimental procedure is based on the well known fact that close to the HDA/LDA transition T_1 of high density amorphous ices is much shorter than that of low density ice.¹⁷ Therefore, T_1 is best suited to monitor the thermal limits of stability.

Fig. 2 presents ^2H spin-lattice relaxation times T_1 obtained by temperature scans of HGW, uHDA, VHDA, eHDA and LDA-II as a function of temperature between 84 K and the respective crystallization temperatures. In all samples, the magnetization recovery is almost monoexponential.

In LDA-II and HGW $T_1(T)$ are almost indistinguishable. Slightly above 135 K, HGW transforms into cubic ice I_c . After crystallization, T_1 in cubic ice (not included in Fig. 2) is about one order of magnitude larger than that of HGW. In contrast,

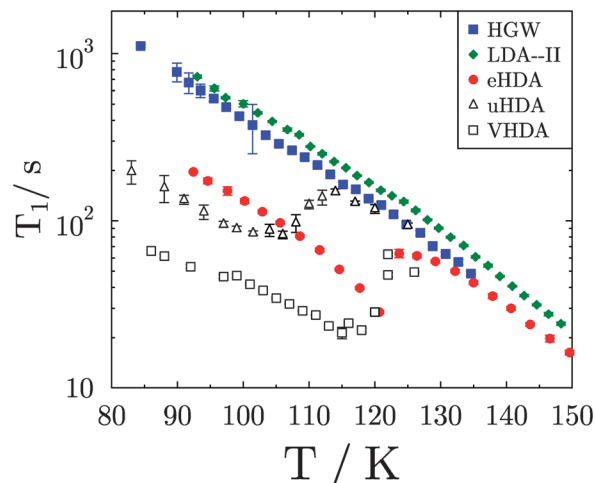


Fig. 2 T_1 of amorphous ices HGW, LDA-II, eHDA, uHDA, VHDA and their transitions to LDA as a function of temperature.

LDA-II is stable up to 150 K and LDA-I produced after heating of uHDA crystallizes to cubic ice I_c at 140 K.¹⁷ Concerning resistance to cubic ice crystallization, we find that among the low density samples LDA-II has a significantly higher thermal stability than HGW. We interpret this in the sense that a small number of (cubic) ice crystallites ($\ll 1\%$ of total sample mass) exist in HGW, which form in the course of the hyperquenching procedure and remain even after annealing at 130 K,²⁰ whereas we regard LDA-II to be void of any crystalline seeds or remnants.¹⁵ Such small ice crystallites may serve as crystallization centers and may lower thermal stability of HGW compared to LDA-II. LDA-II has a thermal stability even higher than that of LDA-I. These findings are in agreement with those of ref. 9 and 16.

At low temperatures, eHDA has shorter ^2H T_1 than the low density forms. At the eHDA/LDA-II transition temperature of 123 K T_1 increases in a significant step. It then joins the temperature dependence of the low density forms, but a slight systematic parallel shift among different LDA-II samples prevails. At 151 K, the sample finally transforms into cubic ice I_c .

To provide a general overview of the transition behaviour of the various high density forms, Fig. 2 also contains the corresponding T_1 data of VHDA and uHDA. While uHDA and VHDA had revealed a strong scatter in absolute T_1 and transition temperatures,¹⁷ we repeatedly performed experiments on various eHDA samples, even from different batches. Nevertheless, we observed strict reproducibility of the absolute T_1 values and the eHDA/LDA-II transition temperature among different batches.

3.2 Sharp eHDA \rightarrow LDA-II transition

Looking back to Fig. 2, we note that the transitions uHDA/LDA-I and VHDA/LDA are rather smooth. On the other hand, the eHDA/LDA-II transition appears to be sharper. This calls for looking at the eHDA/LDA-II transition in more detail.

Fig. 3 shows T_1 and β as a function of temperature for an eHDA/LDA-II sample. In the first scan up to 118 K we avoid the transition to LDA-II. T_1 decreases with increasing temperature while $\beta = 0.89$ remains constant. After cooling back to 93 K, T_1 and β of the second scan match the data of the first scan reasonably well. At 124 K, the magnetization recovery curve can only be fitted with two values of β and T_1 . This indicates that within the duration of one experiment (90 min) the eHDA sample transforms to LDA-II at 124 K. This transition is sharper than those of uHDA and VHDA, see Fig. 2 and ref. 17. LDA-II reveals a stretching parameter β slightly smaller than that of eHDA, see Fig. 3. The sample crystallizes to cubic ice I_c slightly above 150 K.

From our observation of reproducible T_1 values irrespective of repeated heating and quenching and the sharp eHDA/LDA-II transition we conclude that eHDA is the most relaxed high density form of amorphous ice.

3.3 Variability in LDA relaxation

In a quite analogous way, we now ask whether there are progressive annealing phenomena in LDA-II. To this end, we performed a similar temperature scan compared to that shown in Fig. 3. Fig. 4 shows spin–lattice relaxation data of LDA-II that was recovered

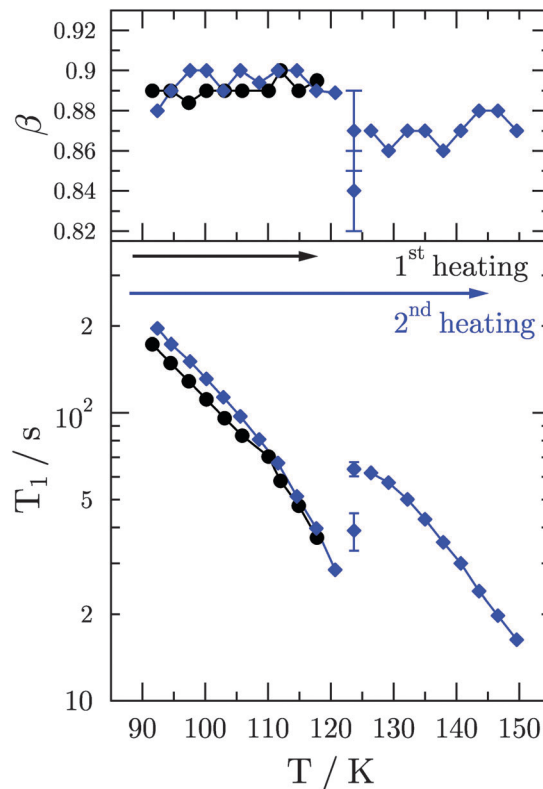


Fig. 3 T_1 and β of eHDA and LDA-II as a function of temperature. The chronology has been as follows: during the first heating (black circles) the temperature is increased in steps of 3 K each 90 min (duration of an experiment) up to 118 K. Then the sample is quenched to 93 K and subsequently heated stepwise again up to the crystallization temperature of 150 K. No error bars are included except for the experiment at the transition temperature of 124 K. Here, the eHDA/LDA-II transition occurred.

from isothermally decompressed VHDA (8 MPa). As explained in the figure caption, we performed three heating cycles. Within the first two heating scans T_1 decreases identically with increasing temperature and the Kohlrausch parameter β remains unchanged. However, above 130 K β drops slightly. Then, during the third upscan, β gets significantly smaller than in the first two scans whereas the absolute T_1 values remain unaffected.

To shed further light on the question of possible irreversible changes in the Kohlrausch parameter, we compare several low density samples with different history (Fig. 5). Here, ^2H T_1 (equivalent to Fig. 2) and β obtained during temperature upscans of HGW and other low density amorphous ices are shown. Since we will discuss the temperature dependence of T_1 in terms of activation energies below (Section 3.4), we choose an Arrhenius type plot where T_1 is plotted logarithmically versus the inverse temperature. The plot reveals that all low density forms possess almost identical spin–lattice relaxation times but differ in the shape of their magnetization recovery curves, *i.e.* there are pronounced and systematic variations in β . Let us briefly go through the samples.

- HGW (■): whereas the T dependence of T_1 does not show anything peculiar, β gradually drops from 0.82 at 90 K to 0.75 at 135 K.

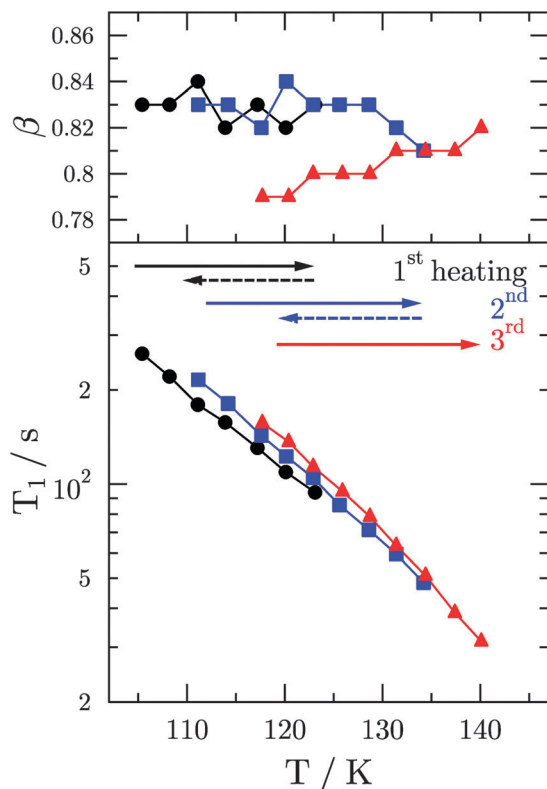


Fig. 4 Temperature dependence of T_1 and β of LDA-II gained from decompressed VHDA. The chronology has been as follows: during the first heating (black circles) the temperature is increased in steps of 3 K each 90 min (duration of an experiment) up to 123 K. Then the sample is quenched to 110 K. In the second scan the sample is heated up to 134 K followed by another quench to 118 K. In the third scan the sample is heated up to 140 K. The error bars of β are of the order of ± 0.01 , and those of T_1 lie within the symbols.

- LDA-II gained from eHDA and subsequently quenched to 89 K (\blacktriangle): the obtained T_1 values are similar to those of HGW. However, the Kohlrausch parameter $\beta \approx 0.81$ is temperature independent.

- LDA-II gained from isothermally decompressed VHDA (8 MPa, two samples \blacklozenge, \circ): again, the temperature dependence of T_1 closely follows that of the previously mentioned samples but the Kohlrausch parameter behaves differently in each case.

Summarizing, since the temperature dependences of T_1 of all above samples are similar to that of HGW, we can indeed consider them as true low density forms. Nevertheless, even the smallest variations in the sample preparation lead to different behaviour as manifested by the Kohlrausch parameter.

3.4 Search for glass transition anomalies

There is a current debate about a possible glass transition of amorphous ice at temperatures above 140 K (see also part I of this twin publication).¹ It is known that a glass transition is manifested in a characteristic increase in the slope of the $\log T_1(T^{-1})$ -dependence as the caloric glass transition temperature T_g is approached from below. This is due to a subtle change in the relaxation mechanism from being dominated by a solid state relaxation mechanism (phonons) at low temperatures to

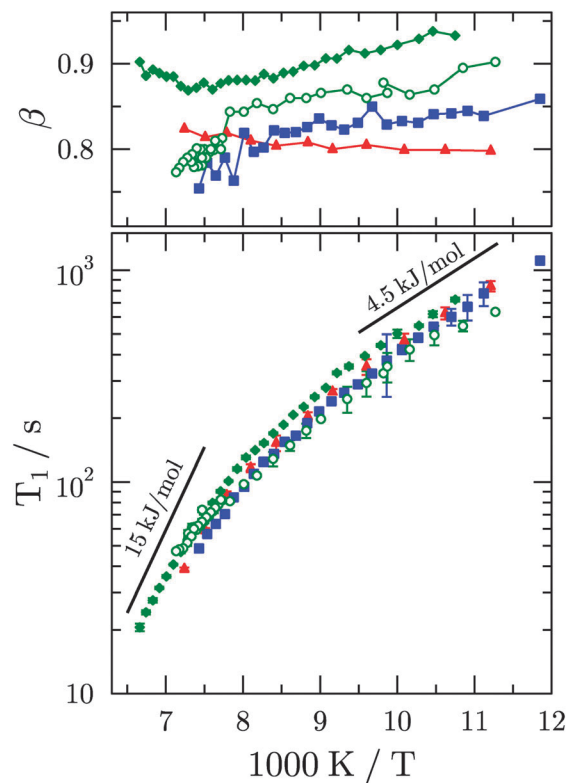


Fig. 5 Temperature dependence of T_1 and β of various low density forms: HGW (\square), LDA-II obtained from eHDA (\blacktriangle), two samples of LDA-II, referred as #1 and #2 (\blacklozenge, \circ), obtained from VHDA decompressed to 8 MPa. In contrast to previous figures, we now choose an inverse temperature scale. Activation energies are indicated in two temperature regions. The two slopes are meant as guides for the eye. The error margins of β can be read from the scatter, the error bars of T_1 are included and lie mostly within the symbols.

molecular dynamics at higher temperatures.^{22–25} Therefore, we inspect Fig. 5 once more.

Indeed, assuming a T -dependence $T_1 \propto \exp[E_A/kT]$ Fig. 5 reveals a sub-Arrhenius behaviour of T_1 with an apparent activation energy E_A , increasing from 4.5 kJ mol⁻¹ at low temperatures towards 15 kJ mol⁻¹ at high temperatures.

As far as β is concerned, one also expects a typical behaviour close to T_g where the molecular system is nonergodic, such that the spin–lattice relaxation is nonexponential ($\beta \approx 0.6$). At even lower temperatures spin diffusion homogenizes the spin system leading to a monoexponential spin–lattice relaxation ($\beta = 1$) again.^{22–25}

4. Conclusions and outlook

²H NMR spin–lattice relaxation parameters present a sensitive tool for the characterization of amorphous ices. Having compared the relaxation behaviour of many different forms of amorphous ice at ambient pressure, we can attribute them to two basic categories, high density and low density forms (see Fig. 8 in ref. 13). As far as the high density forms are concerned, we find strong variations in the relaxation parameters and in their transition temperatures to the low density forms.

This indicates that most of these high density forms are not relaxed or annealed ones. One of these forms, eHDA appears to be best relaxed or most annealed which is experimentally manifested by its reproducible T_1 relaxation times and its sharp transition temperature to LDA-II. In some contrast, the low density amorphous ices exhibit less variations in the ^2H NMR spin–lattice relaxation times. Beyond all common properties, our second NMR parameter, the Kohlrausch exponent β , shows quite erratic variations from one sample to the other. This indicates that sample preparation and sample history lead to subtle variations in the sample properties. One exception may be that in the most relaxed high density form (eHDA) β tends to be larger than in the subsequent low density amorphous ice.

From our results, we can draw no conclusions on the question of the existence of glass transition anomalies. As stated in the Introduction, NMR spin–lattice relaxation probes rather fast processes just as the Debye–Waller factor discussed in part I.¹ By stimulated echo techniques ^2H NMR also has the potential to study ultra slow dynamics, *i.e.* structure relaxation (so-called α -process) of the glass transition. Corresponding work is in progress.

Abbreviations

VHDA	very high density amorphous
eHDA	expanded high density amorphous
uHDA	unrelaxed high density amorphous
rHDA	relaxed high density amorphous
LDA	low density amorphous ice

Acknowledgements

K. Amann-Winkel and T. Loerting are grateful for financial support from the Austrian Science Fund (Firnberg award T463 and START award Y391) and the European Research Council (ERC Starting Grant SULIWA).

References

- 1 K. Amann-Winkel, F. Löw, P. H. Handle, W. Knoll, J. Peters, B. Geil, F. Fujara and T. Loerting, *Phys. Chem. Chem. Phys.*, 2012, **14**, 16386–16391.
- 2 O. Mishima, *J. Chem. Phys.*, 1994, **100**, 5910–5912.
- 3 P. H. Poole, F. Sciortino, U. Essmann and H. E. Stanley, *Nature*, 1992, **360**, 324–328.
- 4 O. Mishima and H. Stanley, *Nature*, 1998, **396**, 329–335.
- 5 C. A. Tulk, C. J. Benmore, J. Urquidi, D. D. Klug, J. Neuefeind, B. Tomberli and P. A. Egelstaff, *Science*, 2002, **297**, 1320–1323.
- 6 M. Koza, H. Schober, H. Fischer, T. Hansen and F. Fujara, *J. Phys.: Condens. Matter*, 2003, **15**, 321–332.
- 7 G. Johari and O. Andersson, *J. Chem. Phys.*, 2004, **120**, 6207–6213.
- 8 M. M. Koza, B. Geil, K. Winkel, C. Kohler, F. Czeschka, M. Scheuermann, H. Schober and T. Hansen, *Phys. Rev. Lett.*, 2005, **94**, 125506.
- 9 K. Winkel, D. T. Bowron, T. Loerting, E. Mayer and J. L. Finney, *J. Chem. Phys.*, 2009, **130**, 204502.
- 10 T. Loerting, C. Salzmann, I. Kohl, E. Mayer and A. Hallbrucker, *Phys. Chem. Chem. Phys.*, 2001, **3**, 5355–5357.
- 11 T. Loerting, W. Schustereder, K. Winkel, C. G. Salzmann, I. Kohl and E. Mayer, *Phys. Rev. Lett.*, 2006, **96**, 025702.
- 12 R. J. Nelmes, J. S. Loveday, T. Strassle, C. L. Bull, M. Guthrie, G. Hamel and S. Klotz, *Nat. Phys.*, 2006, **2**, 414–418.
- 13 T. Loerting, K. Winkel, M. Seidl, M. Bauer, C. Mitterdorfer, P. H. Handle, C. G. Salzmann, E. Mayer, J. L. Finney and D. T. Bowron, *Phys. Chem. Chem. Phys.*, 2011, **13**, 8783–8794.
- 14 K. Winkel, M. Elsaesser, E. Mayer and T. Loerting, *J. Chem. Phys.*, 2008, **128**, 44510.
- 15 M. S. Elsaesser, K. Winkel, E. Mayer and T. Loerting, *Phys. Chem. Chem. Phys.*, 2010, **12**, 708.
- 16 K. Winkel, M. Bauer, E. Mayer, M. Seidl, M. S. Elsaesser and T. Loerting, *J. Phys.: Condens. Matter*, 2008, **20**, 494212.
- 17 M. Scheuermann, B. Geil, K. Winkel and F. Fujara, *J. Chem. Phys.*, 2006, **124**, 224503.
- 18 J. A. Ripmeester, C. I. Ratcliffe and D. D. Klug, *J. Chem. Phys.*, 1992, **96**, 8503.
- 19 E. Mayer, *J. Appl. Phys.*, 1985, **58**, 663.
- 20 I. Kohl, L. Bachmann, A. Hallbrucker, E. Mayer and T. Loerting, *Phys. Chem. Chem. Phys.*, 2005, **7**, 3210.
- 21 K. Schmidt-Rohr and H. W. Spiess, *Multidimensional Solid-State NMR and Polymers*, Academic Press, 1994.
- 22 W. Schnauss, F. Fujara, K. Hartmann and H. Sillescu, *Chem. Phys. Lett.*, 1990, **166**, 381–384.
- 23 W. Schnauss, F. Fujara and H. Sillescu, *J. Chem. Phys.*, 1992, **97**, 1378–1389.
- 24 E. Bartsch, F. Fujara, B. Geil, M. Kiebel, W. Petry, W. Schnauss, H. Sillescu and J. Wuttke, *Physica A*, 1993, **201**, 223–236.
- 25 G. Hinze, G. Diezemann and H. Sillescu, *J. Chem. Phys.*, 1996, **104**, 430–433.